JOURNAL OF CATALYSIS 122, 113–125 (1990)

Effect of Support on the Surface Characteristics of Supported Molybdena Catalysts

C. V. CÁCERES,[1] J. L. G. FIERRO, J. LÁZARO, A. LÓPEZ AGUDO, AND J. SORIA

Instituto de Catálisis y Petroleoquímica, CSIC, Serrano, 119, 28006 Madrid, Spain

Received December 14, 1988; revised September 8, 1989

Various supported molybdena catalysts with submonolayer loading on TiO_2, Al_2O_3, SiO_2, $SiO_2 \cdot Al_2O_3$, and carbon have been prepared by both impregnation and equilibrium adsorption procedures. The characterization of the oxide form of the catalysts by several techniques (X-ray diffraction, XPS, ESR, O_2 chemisorption, and H_2 reduction) revealed that the oxidic Mo phase was highly and homogeneously dispersed, essentially in monolayer form, on TiO_2; well-dispersed and coordinatively heterogeneous on Al_2O_3; and poorly and heterogeneously spread on SiO_2, $SiO_2 \cdot Al_2O_3$, and carbon, in which the presence of three-dimensional MoO_3 crystallites was detected. Catalyst reducibility decreased in the order carbon > $TiO_2 \gg SiO_2 > SiO_2 \cdot Al_2O_3 > Al_2O_3$ for the series prepared by impregnation. For the equilibrium adsorption series, the ranking was very similar except that TiO_2 and carbon changed places. Reducibility was governed by both the Mo dispersion and the molybdena–support interaction which was found to be weaker for TiO_2 and carbon than for Al_2O_3. The conjunction of both high Mo dispersion and weak Mo–support interaction leads generally to high reducibility.

INTRODUCTION

Molybdenum (or tungsten) sulfides promoted with minor amounts of cobalt (or nickel) sulfide supported on transitional aluminas, namely γ- and η-Al_2O_3, constitute the commercial hydrodesulfurization (HDS) catalysts currently in use. One of the most important roles of the alumina is to maintain a high dispersion of the active ingredients on its surface (*1–3*). This is feasible because the surface anionic OH groups of the alumina interact strongly with metal oxides during calcination (*4, 5*), thus causing the extensive spreading of metal oxide over the surface. In the case of molybdenum, this occurs in discrete monolayer patches and/or in the form of small clusters of polymolybdates several layers thick, depending on the loading and the preparation conditions (*6–8*). However, the strong metal oxide–alumina interaction causes an apparent loss of a part of molybdenum and of promoter either into the alumina subsurface or by strong bonding to the alumina surface, making this fraction difficult to sulfide (*9*). Due to this reactivity of alumina, elucidation of the precise structure and nature of HDS active sites of the alumina-supported molybdenum catalysts is difficult since the surface properties of support can affect the structure of the supported molybdenum and promoter species.

This strong metal oxide–alumina interaction together with the need for new and improved hydrotreating catalysts with different distributions of catalytic functionalities has increasingly inspired research in the use of materials different from alumina as supports of molybdenum-based catalysts. Among them, the most extensively studied were, first, the Mo/SiO_2 (see, e.g., Refs. (*10–14*)) system and then the Mo/carbon (*9, 15–20*) system. Both SiO_2 and carbon supports, with high surface areas, are considered relatively inert, giving, therefore, less complex molybdenum catalysts. Despite the apparent inertness of SiO_2 and carbon, it has been shown that quite active HDS

[1] On leave from CINDECA, c/47, No. 257, 1900-La Plata, Argentina.

0021-9517/90 $3.00

catalysts with comparable or higher activity than that on alumina could be prepared on SiO_2 (*18, 21*) and carbon (*9, 16–19*), provided that the Mo loading and the preparation method were appropriate, e.g., organometallic precursors for SiO_2-supported molybdenum catalysts were used (*21*).

More recently, other oxide materials including TiO_2, ZrO_2, and zeolites have attracted much attention as supports of molybdenum catalysts; and several comparative studies with the most conventional Al_2O_3-, SiO_2-, and carbon-supported molybdenum catalysts have been reported (*22–32*). In general, the results on the influence of the support oxide on the surface properties of supported molybdena are varied, and in some cases apparently contradictory, since the comparison is commonly based on preparation of catalysts with equal nominal compositions of molybdenum (*24–29*). For example, the HDS activity for a TiO_2-supported molybdenum (8% Mo) was reported to be low when compared to others on alumina with the same Mo loading (*26*). Later, it was shown (*30*) that the previous finding of less HDS activity for the TiO_2-supported catalysts (*26*) was only valid when the monolayer capacity of TiO_2 was exceeded; at Mo loadings equal or below the monolayer capacity, TiO_2-supported catalysts were more active than the corresponding alumina catalysts. These results show, therefore, the convenience of comparing monolayer-type catalysts (*22, 23*) or preparations with similar coverage, but not exceeding the theoretical monolayer, when fundamental properties of dispersed Mo species on different supports are to be studied. In practice, however, it is extremely difficult to obtain true monolayer-type catalysts containing equal amounts of Mo atoms per unit surface area on different supports from conventional wet impregnation, especially if the support differ largely in isoelectric point (IEP) values. It is well known that the IEP of the support and the pH of the Mo-impregnating solution play a decisive role in the nature of the molybdate species in solution and also in the extent of molybdate anion adsorption (*33*). Adsorption of molybdate anions occurs when the pH of the impregnating solution is below the IEP of the support but, on the contrary, this is not favored when the pH is above the IEP of the support; consequently, the pH value for a favorable adsorption of molybdate anions varies with the type of support. Therefore, homogeneous catalysts, in terms of both loading and dispersion of Mo, cannot be obtained on different support materials by using the same impregnation conditions.

It is the aim of the present work to compare the behavior of several materials of interest, such as Al_2O_3, SiO_2, $SiO_2 \cdot Al_2O_3$, TiO_2, and carbon, as supports of MoO_3. A preliminary account of some of the surface characterization results of a catalyst series in the oxidic form prepared with constant Mo atoms per unit surface area according to conventional impregnation has been previously made (*34*). This has been complemented with XPS and oxygen chemisorption. Also, it has been extended to other catalyst series prepared by an equilibrium adsorption method at pH 10. In this latter case, MoO_3 spreading, mostly in monolayer form, is favored and the Mo–support interaction becomes more predictable.

EXPERIMENTAL

Characteristics of the Supports

The support materials used were commercial Girdler T-126 Al_2O_3, BASF D11-11 SiO_2, Ketjen 3P $SiO_2 \cdot Al_2O_3$ (13.1% Al_2O_3), Degussa T26 TiO_2 (72% anatase), and Girdler G32 coconut carbon. The specific surface areas, obtained according to the BET method from the nitrogen adsorption isotherms at 77 K and a value of 0.163 nm^2 for the cross section of the adsorbed N_2 molecule, are given in Table 1.

The concentration of surface OH groups exchangeable by F^-, i.e., anionic OH, per unit surface area of the support (except for carbon) were measured following the

TABLE 1

Surface Area and OH^- Groups Replaceable by Fluorine of Supports

Support	Surface area ($m^2\ g^{-1}$)	OH^- groups ($mmol \cdot m^{-2} \times 10^3$)
Al_2O_3	188	3.56
SiO_2	123	1.93
$SiO_2 \cdot Al_2O_3$	100	1.99
TiO_2	52	3.10
C	900	—

method of Yamagata *et al.* (*5*). In short, about 1 g of the dried support material was suspended in 25 ml of a 0.057 *M* NH_4F solution, allowed to stand for 24 h, and then filtered. The remaining fluorine in the solution was determined potentiometrically using a fluorine-sensitive electrode. The amounts of surface OH exchangeable by F^- are also summarized in Table 1.

Catalyst Preparation

A molybdena supported catalyst series was prepared by wet impregnation of 25 g of support with 5.0 ml of solution containing stoichiometric amounts of ammonium heptamolybdate (AHM) to achieve the desired Mo loading. As a criterion for catalyst comparison, constant MoO_3 loading per unit surface area on each support and below each theoretical monolayer was considered. The pH values of the AHM solutions were about 6. The excess water was evaporated at 343 K under a pressure of 40 kN m^{-2} in a rotary evaporator. The moist materials were left overnight (15 h) at ambient temperature and then dried at 383 K for 8 h. Finally, the precursors were air-calcined in two steps: 623 K for 2 h and then 773 K for 4 h (except the Mo/C catalyst which was calcined in a N_2 stream). This catalyst series will be referred to hereafter as Mo/*M-I*, *M* = support.

Another molybdena supported catalyst series was prepared by the equilibrium adsorption method at pH 10. First, the supports were contacted at ambient temperature with relatively large volumes of 0.01 *M* AHM solution (a 1 : 20 ratio of support to solution was used). Then, these solutions were shaken mechanically in the Erlenmeyer flask for 24 h. Finally, the excess solution was separated by filtration. The final Mo loading was determined in the preparations by the atomic absorption method. Drying and calcination were the same as above. This latter catalyst series will be referred to hereafter as Mo/*M*-E. The Mo content for all preparations is summarized in Table 2.

TABLE 2

Characterization Data of Supported Molybdena Catalysts

Catalyst	MoO_3 (%)	Mo (Atoms $\cdot$ nm^{-2})	r_0 (813 K) (h^{-1})	BE Mo $3d_{5/2}$ (eV)	O_2 uptake ($mg \cdot g^{-1}$ MoO_3)
Mo/Al_2O_3-I	8.0	1.78	6.00	232.3 (3.7)[a]	72.50
Mo/SiO_2-I	5.2	1.78	18.58	231.9 (3.9)[a]	60.05
$Mo/SiO_2 \cdot Al_2O_3$-I	4.2	1.78	16.22	231.8 (3.8)[a]	76.29
Mo/TiO_2-I	2.1	1.78	433.00	231.7 (1.8)[a]	92.97
Mo/C-I	38.3	1.78	440.40	231.5 (1.7)[a]	27.12
Mo/Al_2O_3-E	1.66	0.37	0.34	—	—
Mo/SiO_2-E	0.95	0.32	3.89	—	—
$Mo/SiO \cdot Al_2O_3$-E	1.14	0.48	1.54	—	—
Mo/TiO_2-E	1.38	1.11	117.60	—	—
Mo/C-E	0.18	0.008	11.58	—	—

[a] Values in parentheses correspond to FWHM in electron volts.

METHODS

X-ray diffraction. The X-ray diffraction patterns were recorded using a Philips PW 1010 vertical diffractometer using nickel-filtered Cu$K\alpha$ radiation, under constant instrumental parameters.

Reduction. The reduction experiments were carried out in a Cahn microbalance connected to a vacuum line and gas-handling system. The samples (ca. 200 mg) were first evacuated at room temperature and then at 393 K to remove the adsorbed water. The temperature was then slowly increased to the desired reduction temperature and maintained until constant weight was achieved. Under these conditions, the samples were contacted with 40 kN m^{-2} of H_2 (99.995% purity) and the kinetic curves of isothermal reduction were recorded. All experiments were conducted under constant H_2 pressure since the dead volume of the microbalance was much larger than the negligible volume of H_2 required for sample reduction. A cold trap at liquid nitrogen temperature (77 K) condensed the water produced in the reduction. The extent of reduction (α) was defined as the ratio of experimental (ΔW_{exp}) to theoretical (ΔW_{the}) weight loss upon reduction,

$$\alpha = \Delta W_{exp}/\Delta W_{the},$$

assuming that all the MoO_3 which contains the catalyst was quantitatively reduced to MoO_2.

Oxygen chemisorption. The extent of oxygen irreversibly chemisorbed on the reduced molybdena catalysts was determined gravimetrically with the same microbalance in each case. The method has been described earlier (*35*). Briefly, the samples previously reduced to almost the same degree of reduction (α = 0.92–1.0) were outgassed under dynamic vacuum ($P < 5 \times 10^{-3}$ N m^{-2}) at 783 K for 3 h and then cooled at 77 K. When steady weight was attained, the samples were contacted with 13.3 kN m^{-2} O_2 until equilibrium was obtained. After this, they were outgassed ($P \sim 1$ N m^{-2}) until constant weight was attained to remove the physically adsorbed O_2.

X-ray photoelectron spectroscopy (XPS). XP spectra were acquired with a Leybold–Heraeus LHS 10 spectrometer equipped with a magnesium anode (Mg$K\alpha$ = 1253.6 eV) operated at 12 kV and 10 mA. The samples were mounted on a sample rod placed in an introduction chamber and pumped to 10^{-3} N m^{-2} for 0.5 h before the sample was moved into the analysis chamber. The pressure in the turbo-pumped analysis chamber was below 8.2×10^{-7} N m^{-2} during data acquisition. At 20 eV, energy regions of the photoelectrons of interest were scanned at a 20-eV spectrometer pass energy, chosen as a compromise enabling acceptable resolution to be obtained within reasonable data acquisition time. C 1*s*, O 1*s*, Mo 3*d*, and Me (Me = Ti 2*p*, Al 2*p*, Si 2*p*) peaks were recorded. All binding energies (BE) were referenced to the adventitious C 1*s* line at 284.6 eV. This reference gave BE values within an accuracy of ±0.2 eV when compared to the Au $4f_{7/2}$ peak at 83.8 eV.

Electron spin resonance (ESR). The ESR spectra were obtained with a Bruker ER 200 D spectrometer operating in the X-band. A modulation of 100 kHz and Mn : MgO (g = 2.0066) standard sample for field calibration was used. The powdered samples (~50 mg) were placed within a vacuum quartz cell assembled with greaseless stopcocks capable of maintaining a dynamic vacuum better than 3×10^{-2} N m^{-2}. Spectra of the catalysts were recorded after vacuum treatment at increasing temperatures from ambient to 773 K for 1 h and then after exposure to H_2 (1.3 N m^{-2}) and heating at different temperatures in the same range for 0.5 h. Both series of spectra, on outgassed and H_2-reduced samples, were recorded at ambient temperature. No significance changes in the Mo^{5+} signal were observed for reduction times longer than 1 h.

RESULTS

X-Ray Diffraction (XRD)

X-ray diffraction patterns for the Mo/Al_2O_3-I and Mo/TiO_2-I catalysts revealed only diffraction lines due to the support structures, whereas for the Mo/$SiO_2 \cdot Al_2O_3$-I, Mo/SiO_2-I, and, particularly, the Mo/C-I catalysts, some diffraction lines characteristic of MoO_3 were clearly observed. The intensity of these lines increased in the order Mo/$SiO_2 \cdot Al_2O_3$-I > Mo/SiO_2-I $\gg$ Mo/C-I. Since the detection limit of this technique for a crystalline phase is about 4 nm, crystallites with sizes larger than this size appeared in the latter catalysts.

Kinetics of Reduction

Typical kinetic curves of isothermal reduction in H_2 at 813 K of catalyst series I and E are shown in Figs. 1a and 1b, respectively. The only exception was the Mo/C-I catalyst for which reduction was measured at 663 K due to its much higher reducibility.

It is clear from Figs. 1a and 1b that the extent of H_2 reduction at 813 K was strongly dependent on the nature of the support and the method of preparation. Thus, e.g., for catalyst series I, the time required to achieve a value of $\alpha = 1.0$ was only a few minutes for the Mo/C-I and Mo/TiO_2-I catalysts, while for Mo/Al_2O_3-I, 5.5 h was necessary. In the case of catalyst series E, the differences in reducibility among all catalysts were even clearer since their reducibility values were relatively lower than those of catalyst series I. For a more precise comparison, e.g., at 813 K, the initial reduction rates of zero time (r_0) were determined by fitting the experimental data of the low-time region of the reduction curves to a hyperbolic function and differentiating at zero time. The r_0 values so obtained are summarized in Table 2.

According to the r_0 values of Table 2, the reducibility of the catalysts decreases in the following order for catalyst series I: Mo/C > Mo/TiO_2 $\gg$ Mo/SiO_2 > Mo/$SiO_2 \cdot Al_2O_3$ > Mo/Al_2O_3. For catalyst series E, it changes slightly: Mo/TiO_2 $\gg$ Mo/C > Mo/SiO_2 > Mo/$SiO_2 \cdot Al_2O_3$ > Mo/Al_2O_3.

It can be seen that both reducibility sequences are quite similar, except for the Mo/TiO_2 and Mo/C catalysts, which are reversed, and also the relatively much higher reducibility of Mo/TiO_2-E compared to the other preparations of series E. These results are slightly different from those reported by Fransen *et al.* (*22, 23*) and by Knözinger *et al.* (*31, 32*) for similar series of molybdena supported catalysts. The differ-

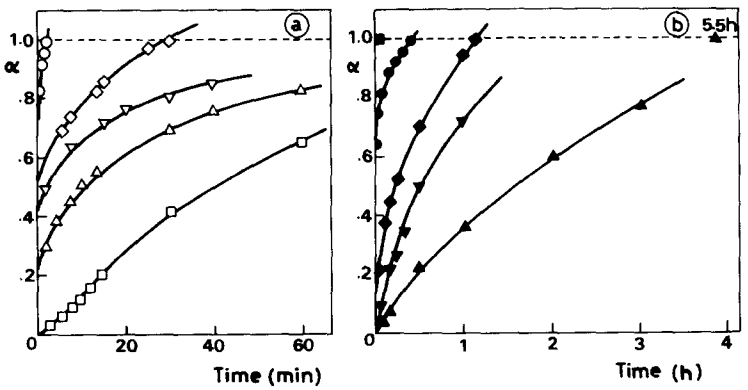

FIG. 1. Kinetics of H_2 reduction at 813 K of supported molybdena catalyst series I (a) and E (b). (○) TiO_2; (◇) SiO_2; (▽) $SiO_2 \cdot Al_2O_3$; (△) Al_2O_3; (□) C. Reduction of MoO_3/C-I catalyst was carried at an exceptionally low (663 K) temperature to make its rate of reduction comparable to that of the other preparations. Open and solid symbols are for catalyst series I and E, respectively.

ences between the previous studies (*22, 23, 31, 32*) and those reported here are probably due to differences in theoretical Mo coverage, methods of catalyst preparation, and reduction procedure, as differences were also observed between the two catalyst series of the present study which differ in both Mo coverage and preparation. Also, differences in reducibility due to different extents of interaction with the support (*36*) are not excluded.

Oxygen Chemisorption

The amount of oxygen irreversibly chemisorbed at 195 K on the reduced (α = 0.92–1.0) molybdena catalyst series I is summarized in Table 2. In the case of catalyst series E, due to the low Mo loading of most of the catalysts, the oxygen uptakes were very small and close to those of the corresponding supports and, hence, very difficult to determine precisely. According to the oxygen uptake (mg of O_2 per g of MoO_3) values of Table 2, the ranking of catalysts in increasing oxygen chemisorption is Mo/C < Mo/SiO_2 < Mo/Al_2O_3 ≈ $Mo/SiO_2 \cdot Al_2O_3$ < Mo/TiO_2.

ESR Spectra

Vacuum pretreatments of the catalysts gave various Mo^{5+} ESR signals of intensity strongly dependent on both temperature and support. The most relevant features of the Mo^{5+} signals are summarized in Table 3. The signal type A, narrow and with low intensity, is observed when the other signals B, C, and D are very weak or absent. Its g-values, lower than g_e, indicate that this is due to trapped electrons, probably in defects in MoO_3. Signal E has been assigned to Mo^{5+} in substitutional positions in TiO_2 (*37*). Signals B, C, and D, generated in most cases by outgassing treatments, show g-values close to those observed by Louis and Che (*38*) for Mo^{5+} in different coordination environments, i.e., signal C to Mo^{5+}_{6c},

TABLE 3

Relevant Features of Mo^{5+} ESR Signals of Outgassed Supported Molybdena Catalysts

Support	A		B		C		D		E or F		
	$g_\perp$	$g_\parallel$	$g_\perp$	$g_\parallel$	$g_\perp$	$g_\parallel$	$g_\perp$	$g_\parallel$	g_1	g_2	g_3
TiO_2			1.958 (at 373 K, intensity maxima at 473 K)	1.853	1.948	1.931	1.955	1.884	1.915 (at room temperature)	1.815	1.790
									1.944 (only after H_2 reduction)	1.938	1.899
SiO_2	1.980 (removed at T > 473 K)	1.959	1.952 (at 773 K)	1.856	1.945 (at 295 K)	1.886	1.955 (H_2 reduction at 773 K)	1.866			
Al_2O_3					1.945 (increases with T_r)	1.872					
$SiO_2 \cdot Al_2O_8$			1.956 (at 773 K)	1.870	1.944 (at 295 K)	1.870					
C	1.977 (only very low intensity A signal)	1.959									

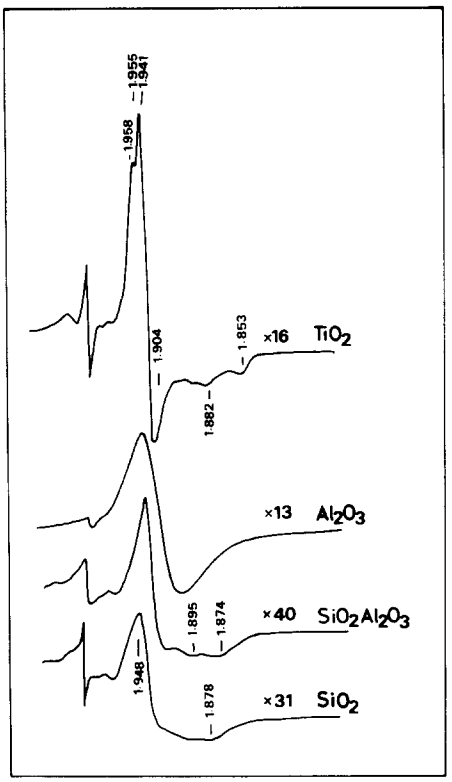

FIG. 2. ESR spectra of catalyst series I after outgassing at 473 K.

signal B to Mo_{5c}^{5+}, and signal D to Mo_{4c}^{5+} ions. Finally, signal F, generated by H_2 treatments, has g-values very close to those of hexacoordinated $Mo^{5+}O_5(OH)$ (*39*).

A comparison of ESR spectra of all series I catalysts, except for Mo/C, outgassed at 473 K, is shown in Fig. 2. The spectrum of the MoO_3/C preparation was not included because the unique type A signal observed had extremely low intensity; even working with very small amounts of sample, a strong microwave absorption by carbon was found. In general, the signals were narrow and well resolved for the Mo/TiO_2 catalysts and broad for Mo/M-I (M = Al_2O_3, SiO_2, $SiO_2 \cdot Al_2O_3$) preparations. The better resolution of the Mo^{5+} ESR signals for TiO_2-supported catalysts suggests good Mo dispersion and a homogeneous oxygen environment around Mo, whereas the broadening of these signals for Al_2O_3, SiO_2, and SiO_2. Al_2O_3-supported catalysts reflect large heterogeneity in the oxygen coordination and probably dipolar magnetic interactions between close Mo^{5+} ions.

After ESR spectra, the same outgassed samples were H_2-reduced at different temperatures in the range T_r = 295–773 K and then the ESR spectra were recorded. The effect of the temperature of reduction on the integrated intensity of the dominant ESR signal per gram of Mo is shown in Fig. 3 for the two catalyst series (I and E). Marked differences in the intensity and dependence on T_r of the signal can be observed among the catalysts. For example, the curve for the Mo/TiO_2-I passed through a maximum at relatively low temperatures (473 K), indicating that the reduction of Mo^{5+} species to Mo^{4+} on the TiO_2 support occurred at very low temperature. By contrast, in the Mo/Al_2O_3-I catalysts, the concentration of Mo^{5+} species is relatively much lower and their detection occurred at higher temperatures (523 K); the maximum concentration shifted to about 673 K. In the

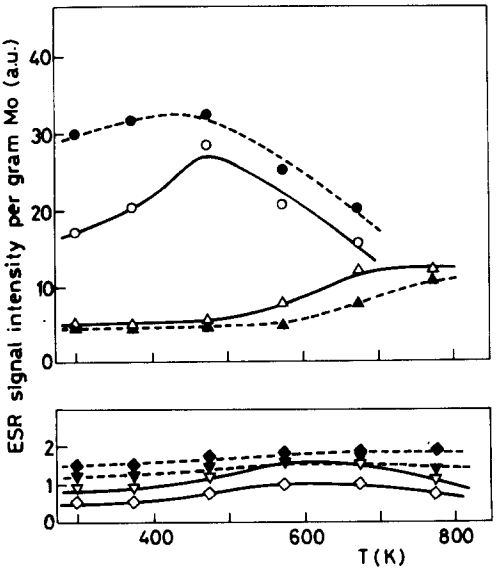

FIG. 3. Variation of the ESR signal intensity (arbitrary units) of the Mo^{5+} signal of H_2-reduced catalysts as a function of the reduction temperature. Symbols have the same meaning as those in Fig. 1.

case of Mo/SiO_2-I and $Mo/SiO_2 \cdot Al_2O_3$-I catalysts, the signal intensities were very low and practically constant with temperature; the appearance of a smooth and broad maximum between 573 and 673 K suggests that most of the Mo^{5+} species formed are rapidly reduced to the lower valence state and/or becomes spin-paired with other Mo^{5+} ions in the MoO_3 cluster.

The Mo/*M* series E catalysts behaved in a similar manner. The signal intensities of series E were slightly lower for $M = TiO_2$ an Al_2O_3 supports and higher for $M = SiO_2$ and $SiO_2 \cdot Al_2O_3$ supports than those of the analogous catalyst counterparts in series I. In general, the most significant difference was that the Mo^{5+} signal intensity began to increase at a higher T_r for catalyst series E; this was particularly clear for the Mo/Al_2O_3-E catalyst, which showed the Mo^{5+} ESR signal increase to occur at ca. 100 K higher T_r than that of its Mo/Al_2O_3-I catalyst counterpart.

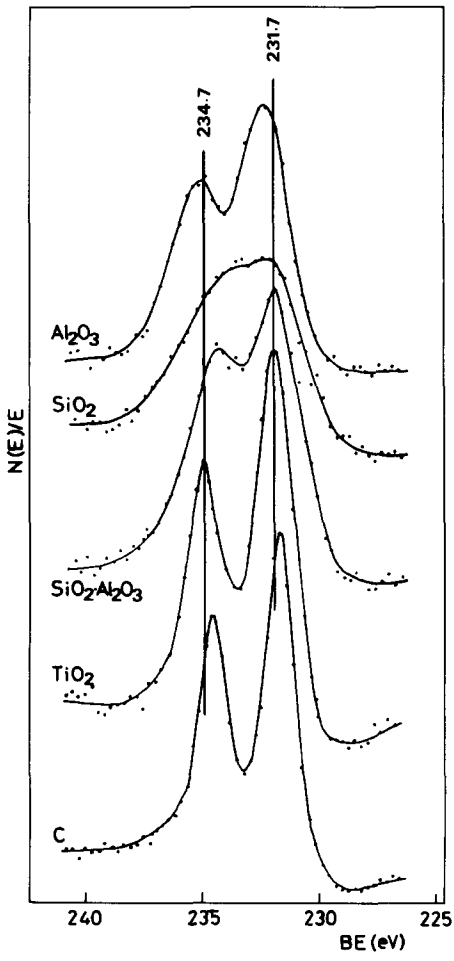

FIG. 4. XPS spectra of the Mo $3d_{5/2}$ and Mo $3d_{3/2}$ levels of the different supported molybdena catalysts of series I.

Photoelectron Spectra (XPS)

Photoelectron spectra of the Mo $3d_{5/2}$ and Mo $3d_{3/2}$ levels of Mo/*M* ($M = Al_2O_3$, SiO_2, $SiO_2 \cdot Al_2O_3$, TiO_2, and C) catalysts of series I are given in Fig. 4. The Mo $3d_{5/2}$ BE and the full width at half maxima (FWHM) values are given in Table 2. As can be seen, both BE and FWHM were largely influenced by the nature of the support surface. For instance, the low FWHM values (1.7–2.0 eV) found on the TiO_2 and C supports contrast clearly with the rather high values (above 3.7 eV) observed on the Al_2O_3, SiO_2, and $SiO_2 \cdot Al_2O_3$ supports. The poorer resolution of the Mo 3*d* doublet in the Mo/SiO_2-I preparation should be noted. In this case, the spectrum is rather complicated since it contains a certain contribution of Mo^{5+} species together with the major Mo^{6+} species. This finding is in agreement with the bluish color of the sample observed after X-ray irradiation. The formation of "molybdenum blue oxides" is associated with the appearance of molybdenum suboxides ($Mo^{\delta+}$; $5 < \delta < 6$), due to the removal of some lattice oxygen of the MoO_6 octahedra and further rearrangement of the defective structures under exposure of the sample to the X-ray beam. Note also that if the Mo 3*d* doublet of the Mo/TiO_2-I catalyst is taken as reference (Mo $3d_{3/2}$ = 234.7 eV and Mo $3d_{5/2}$ = 231.7 eV) a slight shift toward higher BE was observed for the Mo 3*d* levels in the Mo/Al_2O_3-I catalyst, while an opposite shift toward lower BE was found in the Mo/C-I catalyst. No reference is made to the Mo/SiO_2-I and $Mo/SiO_2 \cdot Al_2O_3$-I catalysts due to the uncertainty of the precise determination of the

BEs of the Mo 3*d* levels. The observed shift toward higher BE of the Mo 3*d* levels in the Mo/Al_2O_3-I catalyst provides evidence for a strong interaction between the Mo layer and the support surface in calcined preparations. The reason for the opposite shift in the Mo/C-I catalyst may, however, lie in the semiconductor character of the carbon support.

To gain an insight into the relative abundance of the Mo species at the surface of these supports, the Mo 3*d*/Me = Al 2*p*, Si 2*p* (for SiO_2 and $SiO_2 \cdot Al_2O_3$), Ti 2*p*, and C 1*s* intensity ratios were measured. These ratios were compared to the corresponding Mo/Me bulk ratios in Fig. 5. This figure also summarizes the theoretical Mo/Me intensity ratios calculated according to the Kerkhoff–Moulijn model (*40*), in which monolayer coverage of the carrier surface is assumed. In this calculation, Scofield's (*41*) photoionization cross sections and the escape depths of the electrons derived from Penn (*42*) were used. Since these parameters are not available for $SiO_2 \cdot Al_2O_3$ support, they were estimated assuming an additive behavior of the SiO_2 and Al_2O_3 components. It is interesting to note that the experimental XPS Mo/Me intensity ratio, compared to the theoretical intensity ratio, was similar for TiO_2 and slightly lower for Al_2O_3 supports, while they become markedly lower for $SiO_2 \cdot Al_2O_3$ and much lower for SiO_2 supports. On the other hand, the C support shows an opposite deviation. This particular behavior of the latter preparations may lie in the formation of shell-type preparations induced by the particular characteristics of this support, viz., microporosity.

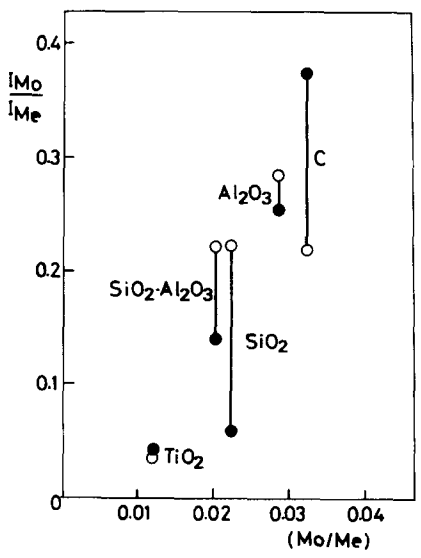

FIG. 5. Comparison of the experimental (●) Mo/*M* XPS intensity ratios and those predicted by the Kerkhoff and Moulijn model (*40*) for monolayer-type molybdena supported catalysts (○) versus the chemical Mo/*M* ratios for the MoO_3/*M*-I catalyst series.

DISCUSSION

The above characterization results reveal important differences in surface distribution of Mo species among the catalysts of series I, although all of them were theoretically prepared with a constant surface density of 1.78 Mo atoms per nm^2, which corresponds to less than 50% of the theoretical complete monolayer (*22, 23*) capacity of each support (*24, 25, 43*). The XRD patterns of the Mo/Al_2O_3-I and Mo/TiO_2-I catalysts were virtually identical to those of their support precursors, and the experimental XPS Mo/Al and Mo/Ti intensity ratios (Fig. 5) were very close to the theoretical monolayer intensity ratios, indicating that molybdena is, in principle, highly dispersed on TiO_2 and well-dispersed on Al_2O_3, in agreement with the literature (see, e.g., Refs. (*1–3, 30–32, 43*)). The slight deviation of the experimental Mo/Al intensity ratio from the calculated monolayer ratio seems to be within the experimental error for quantitative XPS measurements. On the contrary, the experimental XPS Mo/Si intensity ratios for the Mo/SiO_2-I and $Mo/SiO_2 \cdot Al_2O_3$-I catalysts were lower, ca. 60 and 30%, respectively, than those for the monolayer values, indicating that molybdena is poorly dispersed on $SiO_2 \cdot Al_2O_3$, and particularly on SiO_2. This is in line with the observation of XRD diffraction lines due to crystalline MoO_3 in

such catalysts, which are more intense in the Mo/SiO_2-I catalyst. In the case of the Mo/C-I catalyst, the Mo/C intensity ratio was, however, considerably higher (~70%) than the theoretical ratio for a uniform monolayer coverage. This deviation indicates that the Mo phase is inhomogeneously dispersed on the carbon surface, with an enrichment of Mo at the outer surface of the support grains, in some regions forming bulk MoO_3, as XRD clearly showed. The enrichment of Mo at the outer surface of the carbon grains is probably caused (i) by the high MoO_3 loading (38.3 wt%) incorporated to the carbon in order to adequately compare the different catalysts (1.78 Mo atoms per nm^2), and (ii) by the relatively very high proportion of narrow micropores present in carbon compared with that in the other supports. It is likely that such narrow micropores prevent diffusion of molybdate during the impregnation step. Another factor contributing to the inhomogeneous distribution of MoO_3 is probably the weak molybdate–carbon surface interaction. During the aqueous impregnation, an important part of molybdate remains in the solution filling the pores, which will consequently lead to transport of these species from the inner pores toward the outer part of the support grains during the drying step. A similar effect of metal enrichment at the outer surface has been reported for carbon–support transition metal sulfides (*9*).

The present results of surface concentration of anionic hydroxyl groups summarized in Table 1 are, in general, consistent with the extent of Mo dispersion determined by XPS. The two supports with higher amounts of OH groups, Al_2O_3 and TiO_2, present the higher Mo dispersion degree according to XPS, which is in accordance with the well-known interaction process between molybdate and alumina proposed by Dufaux *et al.* (*4*), extensible also to other supports with surface OH groups. However, closer comparison of the data indicates that the number of OH groups is not the only factor determining Mo dispersion; the M–OH bond strength seems to be also important. For example, the amount of OH in SiO_2 is nearly one-half of that in Al_2O_3, but the former support shows little evidence of molybdate–SiO_2 interaction because SiOH is too strong; consequently SiO_2 is considerably less effective for dispersing molybdate. Another factor which influences the molybdate spreading, particularly important for the Mo distribution and the type of Mo species, is the distribution of surface OH groups in supports. This is the case of Al_2O_3 and TiO_2 supports, which presented roughly comparable surface concentrations of anionic OH groups (Table 1), but are uniformly distributed on the TiO_2 surface (*44, 45*) and in parallel rows on the Al_2O_3 surface (*46*). This difference between Al_2O_3 and TiO_2 is reflected in a different distribution of Mo on each support, as previously suggested (*30*), and as the differences found between the ESR and XPS spectra of Mo/Al_2O_3-I and Mo/TiO_2-I catalysts also suggest. Thus, the Mo^{5+} ESR signals appeared relatively well-resolved for Mo/TiO_2-I and broad for Mo/Al_2O_3-I, indicating a higher homogeneity in the coordination of the molybdena supported on TiO_2 than that on Al_2O_3. This difference in Mo distribution is corroborated by the XPS spectra of Fig. 4. The Mo 3*d* doublet for Mo/TiO_2-I presented excellent resolution and a lower FWHM value (1.8 eV) compared with that of Mo/Al_2O_3-I (3.7 eV), suggesting also that Mo species on TiO_2 are more homogeneously distributed and more similarly chemically coordinated, whereas on Al_2O_3 Mo^{6+} species with different chemical characteristics are present. Recently, Ng (*47*) has observed similar differences in XPS results comparing TiO_2- and Al_2O_3-supported molybdena catalysts and also concluding that the dispersed MoO_3 phase on TiO_2 has more uniform geometrical and chemical characteristics than that on Al_2O_3.

The reducibility results provide further insight into the dispersion and nature of the

supported MoO_3 species. Reducibility is largely governed by the extent of Mo dispersion, by the type of Mo species, i.e., tetrahedrally coordinated (Mo_T) or octahedrally coordinated (Mo_O), and by the MoO_3–support interaction. Bulk MoO_3 is more easily reduced than supported molybdena, and weakly bonded molybdena is more easily reduced than strongly bound molybdena species (*36*). Accordingly, Table 2 shows that the lowest reducibility value corresponds to the Mo/Al_2O_3-I catalyst, which possesses a relatively high Mo dispersion and a strong molydena–Al_2O_3 interaction. On the other extreme is the Mo/C-I catalyst. This catalyst has a considerably high reducibility value, reflecting the presence of MoO_3 crystallites, together with another fraction of MoO_3 satisfactorily dispersed and very weakly bonded Mo species on the carbon surface. The Mo/TiO_2-I also showed a reducibility value comparable to that of Mo/C-I; this can be explained by the high dispersion of Mo on TiO_2, by a higher fraction of polymeric Mo_O, and by a weaker interaction between molybdena and TiO_2 compared with that with Al_2O_3 and possibly with $SiO_2 \cdot Al_2O_3$ and SiO_2. Thus, the conjunction of a high Mo dispersion and a weak Mo–support interaction also facilitates the Mo reduction. For the Mo/SiO_2-I and $Mo/SiO_2 \cdot Al_2O_3$-I catalysts the reducibility values were moderately low, although slightly higher than for Mo/Al_2O_3-I. In these catalysts Mo is poorly dispersed, as derived from XRD and XPS results, but interaction between supported molybdate and $SiO_2 \cdot Al_2O_3$ is probably stronger than that for carbon, although weaker than that for Al_2O_3. However, more reliable information on Mo–support interaction is expected to be obtained by comparing the reducibility values of catalyst series E, in which the Mo loadings were generally lower and the preparation conditions may favor the formation of a monolayer-type structure. In these preparations the reducibility is then essentially governed by the Mo–support interaction. Indeed, with the exception of the Mo/TiO_2-E catalyst, the values of r_0 of Table 2 are consistent with the above findings on the strength of the Mo–support interaction. The exceptionally high reducibility of Mo/TiO_2-E points out that supported Mo species may interact relatively more weakly on the surface of TiO_2 than on Al_2O_3. This is also shown by the ESR results of Fig. 3, where it can be seen that for the Mo/TiO_2 preparations the Mo reduction progresses easily to Mo^{4+} or lower valence state still at a relatively low temperature (573 K). This exceptionally high reducibility of Mo/TiO_2-E compared with that of Mo/C-E could be due to the difference in Mo loading, which is relatively much lower for Mo/C-E than for Mo/TiO_2-E. Because on carbon the Mo loading is extremely low, the supported MoO_3 phase consists probably of isolate Mo_T species, while on TiO_2 the presence of polymeric Mo_O species is more likely due to the Mo loading. Some contribution of the reduction of TiO_2 support to the overall reduction of Mo/TiO_2 catalyst is not excluded. In order to quantify the contribution of the support, a blank experiment with TiO_2 alone showed some reduction, although the kinetic curve of reduction was much more retarded than that of the Mo/TiO_2 catalyst.

The observed differences in molybdena dispersion, as derived from quantitative XPS results, are qualitatively maintained, except for Mo/Al_2O_3-I, in their reduced state according to the O_2 chemisorption results of Table 2. The low O_2 chemisorption values for Mo/C-I and Mo/SiO_2-I are in line with the presence of large MoO_3 crystallites on carbon and SiO_2 and, therefore, with low concentrations of exposed coordinately unsaturated Mo sites (CUS) able to adsorb O_2, generated upon H_2 reduction. For $Mo/SiO_2 \cdot Al_2O_3$, and particularly for Mo/TiO_2-I, the O_2 uptakes were higher, reflecting the increase in MoO_3 dispersion shown by XPS. However, these increases are not similar for both techniques. The discrepancy between MoO_3 dispersion derived by XPS and O_2 chemisorption is clearer

when Mo/TiO_2-I and Mo/Al_2O_3-I are compared. According to XPS the Mo dispersion is comparable for both Mo/TiO_2-I and Mo/Al_2O_3-I, while according to O_2 chemisorption the later results in lower Mo dispersion, virtually similar to that for $Mo/SiO_2 \cdot Al_2O_3$. This difference can be attributed either to a change or rearrangement of MoO_3 crystals during H_2 reduction or to differences in the distribution of MoO_3 between Al_2O_3 and TiO_2 (discussed above) such that it determines the formation of CUS. The first explanation seems to be unlikely since the weaker interaction between MoO_3 and TiO_2 (relative to the MoO_3/Al_2O_3 system) would lead to some aggregation of MoO_3 during reduction and, hence, to a lower Mo dispersion by O_2 chemisorption compared with Mo/Al_2O_3-I, in which such an effect is unlikely due the strong MoO_3–Al_2O_3 interaction. Rather, the minor O_2 chemisorption of Mo/Al_2O_3-I relative to the Mo/TiO_2-I catalyst is related to both the Mo distribution and the MoO_3–support interaction. As Mo is spread more uniformly on TiO_2 than on Al_2O_3 surfaces it is expected that the size of monolayer patches may be lower on TiO_2. In this respect it is noted that Ng and Gulari (*30*) observed that for the Mo/TiO_2 system multilayer patches and bulk MoO_3 can be formed only when monolayer coverage is exceeded, while for the Mo/Al_2O_3 system MoO_3 formation can be detected even at submonolayer loadings.

ACKNOWLEDGMENTS

This work was supported by CAICYT (Spain). One of us (C.V.C) thanks CONICET (Argentina) for a fellowship.

REFERENCES

1. Massoth, F. E., *in* "Advances in Catalysis" (D. D. Eley, H. Pines, and P. B. Weisz, Eds.), Vol. 27, p. 265. Academic Press, San Diego, 1978.
2. Delmon, B., *in* "Proceedings of the Climax Third International Conference on the Chemistry and Uses of Molybdenum" (H. F. Barry and P. C. H. Mitchell, Eds.), p. 343. Climax Molybdenum Co., Ann Arbor, MI, 1982.
3. Grange, P., *Cat. Rev. Sci. Eng.* **21,** 135 (1980).
4. Dufaux, M., Che, M., and Naccache, C., *J. Chim. Phys.* **67,** 527 (1970).
5. Yamagata, N., Owada, Y., Okazaki, S., and Tanabe, K., *J. Catal.* **47,** 358 (1977).
6. Wang, L., and Hall, W. K., *J. Catal.* **66,** 251 (1980).
7. Jeziorowski, H., Knözinger, H., Taglauer, E., and Vogdt, C., *J. Catal.* **80,** 286 (1983).
8. Gil-Llambías, F. J., Escudey-Castro, A. M., López Agudo, A., and Fierro, J. L. G., *J. Catal.* **90,** 323 (1984).
9. Groot, C. K., Van der Kraan, A. M., de Beer, V. H. J., and Prins, R., *Bull. Soc. Chim. Belg.* **93,** 707 (1984), and references therein.
10. Gajardo, P., Declerck-Grimée, R. I., Delvaux, G., Olodo, P., Zabala, J. M., Canesson, P., Grange, P., and Delmon, B., *in* "Proceedings of the Climax Second International Conference on the Chemistry and Uses of Molybdenum" (P. C. H. Mitchell, Ed.), p. 150. Climax Molybdenum Co., London, 1977.
11. de Beer, V. H. J., van der Aalst, M. J. M., Machiels, C. J., and Schuit, G. C. A., *J. Catal.* **43,** 78 (1976).
12. Gajardo, P., Grange, P., and Delmon, B., *J. Phys. Chem.* **83,** 1771 (1979).
13. Topsøe, H., Clausen, B. S., Burriesai, N., Candia, R., and Mørup, *in* "Preparation of Catalysts, II" (B. Delmon, P. Grange, P. Jacobs, and G. Poncelet, Eds.), p. 479. Elsevier, Amsterdam, 1979.
14. Jeziorowski, H., Knözinger, H., Grange, P., and Gajardo, P., *J. Phys. Chem.* **84,** 1825 (1980).
15. Stevens, G. C., and Edmonds, T., *in* "Preparation of Catalysts, II" (B. Delmon, P. Grange, P. Jacobs, and G. Poncelet, Eds.), p. 507. Elsevier, Amsterdam, 1979.
16. Breysse, M., Bennet, B. A., Chadwick, D., and Vrinat, M., *Bull. Soc. Chim. Belg.* **90,** 1271 (1981).
17. de Beer, V. H. J., Duchet, J. C., and Prins, R., *J. Catal.* **72,** 369 (1981).
18. Duchet, J. C., van Oers, E. M., de Beer, V. H. J., and Prins, R., *J. Catal.* **80,** 386 (1983).
19. Vissers, J. P. R., de Beer, V. H. J., and Prins, R., *Faraday Symp. Chem. Soc.* paper 15, **21** (1986).
20. Bridgewater, A. J., Burch, R., and Mitchell, P. C. H., *Appl. Catal.* **4,** 267 (1982).
21. Yermakov, Y. I., Startsev, A. N., and Burmistrov, V. A., *Appl. Catal.* **11,** 1 (1984).
22. Fransen, T., van Berge, P. C. and Mars, P., *in* "Preparation of Catalysts, I" (B. Delmon, P. A. Jacobs, and G. Poncelet, Eds.), p. 405. Elsevier, Amsterdam, 1976.
23. Fransen, T., Mars, P., and Gellings, P. J., *J. Colloid Interface Sci.* **70,** 97 (1979).
24. Hattori, H., Tanabe, K., Tanaka, K., and Okazaki, S., *in* "Proceedings of the Climax Third International Conference on the Chemistry and Uses of Molybdenum" (H. F. Barry and P. C. H. Mitchell, Eds.), p. 188. Climax Molybdenum Co., Ann Arbor, MI, 1979.

25. Swanson, W. W., Strensand, B. J., and Tsigdinos, G. A., *in* "Proceedings of the Climax 4th International Conference on the Chemistry and Uses of Molybdenum (H. F. Barry and P. C. H. Mitchell, Eds.), p. 323. Climax Molybdenum Co., Ann Arbor, MI, 1982.
26. Muralidhar, G., Massoth, F. E., and Shabtai, J., *J. Catal.* **85,** 44 (1984); *J. Catal.* **85,** 53 (1984).
27. Kohno, T., Yokono, T., Sanada, Y., Yamashita, K., Hattori, H., and Makino, K., *Appl. Catal.* **22,** 201 (1986).
28. Nishijima, A., Shimada, H., Sato, T., Yoshimura, Y., and Hiraishi, J., *Polyhedron* **5,** 243 (1986).
29. Cid, R., Villaseñor, J., Orellana, F., Fierro, J. L. G., and López Agudo, A., *Appl. Catal.* **18,** 357 (1985).
30. Ng, K. Y. S., and Gulari, E., *J. Catal.* **92,** 340 (1985); *J. Catal.* **95,** 33 (1985).
31. Leyrer, J., Vielhaber, B., Zaki, M. I., Zhuang, S., Weitkamp, J., and Knözinger, H., *Mater. Chem. Phys.* **13,** 301 (1985).
32. Zaki, M. I., Vielhaber, B., and Knözinger, H., *J. Phys. Chem.* **90,** 3176 (1986).
33. Wang, L., and Hall, W. K. *J. Catal.* **77,** 232 (1982).
34. Cáceres, C. V., Fierro, J. L. G., López Agudo, A., and Soria, J. A., *in* "Proceedings, 10th Iberoamerican Symposium on Catalysis, Mérida, Venezuela, 1986," p. 207.
35. López Agudo, A., Gil-Llambias, F. J., Reyes, P., and Fierro, J. L. G., *Appl. Catal.* **1,** 59 (1981).
36. Massoth, F. E., *J. Catal.* **30,** 204 (1973).
37. Kyi, R., *Phys. Rev.* **128,** 151 (1962).
38. Louis, C., and Che, M., *J. Phys. Chem.* **91,** 2875 (1987).
39. Yamazoe, T., *J. Chem. Soc. Dalton Trans.*, 1987 (1982).
40. Kerkhoff, F. P. J. M., and Moulijn, J. A., *J. Phys. Chem.* **83,** 1612 (1979).
41. Scofield, J. H., *J. Electron Spectrosc. Relat. Phenom.* **8,** 129 (1976).
42. Penn, D. R., *J. Electron Spectrosc. Relat. Phenom.* **9,** 29 (1976).
43. Liu, Y. C., Griffin, G. L., Chan, S. S., and Wachs, I. E., *Appl. Catal.* **94,** 108 (1985).
44. Boehm, H. P., in "Advances in Catalysis" (D. D. Eley, Herman Pines, and Paul B. Weisz, Eds.), Vol. 16, p. 179. Academic Press, New York, 1966.
45. Boehm, H. P., and Hermann, M., *Z. Anorg. Allg. Chem.* **352,** 156 (1976); *Z. Anorg. Allg. Chem.* **368,** 73 (1969).
46. Knözinger, H., and Ratnasamy, P., *Catal. Rev. Sci. Eng.* **17,** 31 (1978).
47. Ng, N. K., *Phys. Chem.* **91,** 2324 (1987).